

# A Novel Method for Vessel Segmentation and Automatic Diagnosis of Vascular Stenosis

Chenxin Sui<sup>1</sup>, Zhuang Fu<sup>1</sup>, Zeyu Fu<sup>1</sup>, Yao Wang<sup>1</sup>, Yu Zhuang<sup>1</sup>,  
Rongli Xie<sup>2</sup>, Yanna Zhao<sup>3</sup>, Jun Zhang<sup>2</sup> and Jian Fei<sup>2</sup>

**Abstract**—A novel method of vessel segmentation in angiography image processing is studied. The process of vessel segmentation is implemented based on Hessian matrix, in which a new vascular function is employed. Subsequently, the vessel contour is extracted from the handled image by using the dual-stage region growing. Extracting vessel skeleton, searching skeleton point and measuring diameter are carried out to realize the automatic diagnosis of vascular stenosis based on vessel segmentation. The experimental results show that the stated method for vessel segmentation manages to accurately extract the main branch contour, and even most small vessels. The automatic diagnosis of vascular stenosis can get relatively accurate results, which may provide auxiliary references and quantify the judgment of vascular stenosis for doctors.

**Index Terms**—vessel segmentation, automatic diagnosis, angiographic images

## I. INTRODUCTION

With the aging of the population and the urbanization accelerating in recent years, the prevalence of cardiovascular diseases (CVD) in China has increased by years. According to the relevant data of “Summary of the 2018 Report on Cardiovascular Diseases in China”, cardiovascular disease was the leading cause of death among urban and rural residents in 2016. The mortality of CVD accounted for more than 40% of all deaths. According to the data, the number of patients with cardiovascular disease is about 290 million, and the prevalence rate is still rising [1]. Thus, the diagnosis and treatment of cardiovascular diseases is significant. X-ray angiography is a common method for diagnosing cardiovascular diseases [2]. The traditional diagnosis process is that the doctor directly observes the angiographic image, and diagnoses according to his/her own experience. It leads some problems. When large number of angiographic images are handled, it requires much more time, and the accuracy of the diagnosis is greatly affected by personal experience. Moreover, the lesion could not be described quantitatively.

<sup>1</sup>C. Sui, Z. Fu, Z. Y. Fu, Y. Wang and Y. Zhuang are with State Key Lab of Mechanical System and Vibration, Shanghai Jiao Tong University, Shanghai 200240, China (e-mail: {jason.sui, zhfu, summer0528, sjtuyao}@sjtu.edu.cn, zhuangyu68@126.com).

<sup>2</sup>R. Xie, J. Zhang and J. Fei are with Ruijin Hospital affiliated to Shanghai Jiao Tong University School of Medicine, Shanghai 200025, China (e-mail: rongli.xie@hotmail.com, 13816000547@163.com, feijian@hotmail.com).

<sup>3</sup>Y. Zhao is with Shanghai Ruijin Rehabilitation Hospital, Shanghai 200023, China (e-mail: zhaoyanna321@sina.com).

Recently, intelligent medical image recognition develops rapidly. The use of image processing technology for auxiliary analysis of angiographic images can quickly and accurately segment the vascular structure and identify suspicious lesions in the blood vessels, which can greatly reduce the burden on doctors and improve the reliability of diagnosis.

Vessel segmentation is the fundamental of angiographic image processing, and is also the theoretical basis for three-dimensional reconstruction of blood vessels, quantitative analysis, and surgical navigation [3]. In recent years, various methods for applying vessel segmentation have been proposed. In Ref. [4], Li et al. adopted the algorithm based on the Markov random field, realized retinal vessel segmentation by calculating the maximum posterior probability. It had good segmentation effect, but ignored the tests of lesion and complicated condition. Lv et al. [5] adopted the center-line constrained level set algorithm for vessel segmentation, which improved the identification accuracy and level set evolution. It could be applied to 2D and 3D data as well. However, the algorithm failed to achieve the extraction of the narrow endings in vascular structure. Roy et al. [6] proposed a method based on Clifford algebra for vessel segmentation in fundus image. This method is fast with higher accuracy but does not consider very thin vessel edge affecting the value of sensitivity. Li et al. [7] presented a wide and deep neural network with strong induction ability to model the transformation to realize the vessel segmentation in retinal images with high accuracy and robustness, and even micro vessels with low contrast are classified precisely. Fu et al. [8] proposed a retinal vessel segmentation based on deep learning architecture and fully-connected CRFs, with high accuracy, and utilized learned discriminative features to deal with challenge of many false positive pixels. However, they both need a large number of training samples and long period of training. In terms of detection of coronary artery stenosis, Chen et al. [9] used the level set algorithm and the local minimum point method to realize the automatic identification of vascular stenosis after vessel segmentation, which had a good grading effect. However, there were some problems such as misjudgment in moderate and severe stenosis segments.

In order to segment the effective blood vessel contour, this paper adopts a new vascular function based on multi-scale enhancement, and multi-stage region growing is employed

subsequently. On the vascular skeleton extraction which is based on the Zhang-Suen algorithm [10], the diameter of the blood vessel is calculated point by point from the segmented blood vessel, and whether the vascular obstruction or lesion exists in this part will be automatically detected.

The rest of this paper is organized as follows. In Section II, the methodology of the proposed work will be discussed, followed by Section III, which illustrates the design and the results of the experiment. Section IV will present the conclusion, including some limitations and future work finally.

## II. PROPOSED METHOD

Vessel segmentation and stenosis recognition will be illustrated in this section. A new approach for vessel segmentation has been studied, which will be specifically illustrated as following procedure, multi-scale vascular enhancement and dual-stage region growing. Based on the Zhang-Suen algorithm, skeleton extraction of blood vessel images is carried out, and the diameter of blood vessel is calculated point by point and the obstruction situation is detected in segments, so as to realize the automatic diagnosis of stenosis.

### A. Vessel Segmentation

1) *Multi-scale Vascular Enhancement*: The blood vessel has a linear tubular structure in the contrast image, and the Hessian matrix-based enhancement filter is commonly used to enhance the blood vessel. The original Hessian matrix of the two-dimensional image  $I$  is defined as

$$H(p) = -\partial^2 I = \begin{bmatrix} I_{xx} & I_{xy} \\ I_{yx} & I_{yy} \end{bmatrix}. \quad (1)$$

Where  $I_{xx}$ ,  $I_{xy}$ ,  $I_{yx}$  and  $I_{yy}$  is the second-order reciprocal of the image. The Hessian matrix of the image is a real symmetric matrix whose eigenvectors are perpendicular to each other. The maximum eigenvalue and corresponding eigenvectors represent the intensity and direction of the maximum curvature of the three-dimensional surface. The eigenvectors corresponding to the smaller eigenvalues represent the direction perpendicular to the maximum curvature.

Since the noise has a great influence on the second-order differential of the image, and the diameter scale of the blood vessel is different, simply using the above formula cannot have a great influence on the blood vessels of various scales [12]. Therefore, equation (1) is transformed to

$$H(p, \sigma) = \sigma^2 \cdot (-\partial^2 G_\sigma) \otimes I. \quad (2)$$

Where the Gaussian function is

$$G_\sigma = \exp\left(-\frac{x^2 + y^2}{2\sigma^2}\right). \quad (3)$$

$\sigma$  is a spatial scale factor. By changing  $\sigma$  blood vessels of different sizes can be enhanced. The  $\sigma^2$  term in (2) is used to normalize the response of each scale.

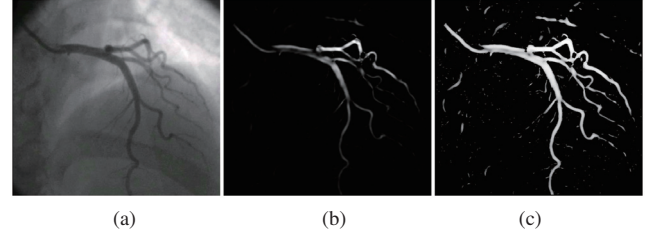


Fig. 1. Contrast of enhancement effects of different vascular functions is shown on angiographic images. (a) Original angiographic images. (b) Enhancement effect of Frangi vascular function. (c) Enhancement effect of the new vascular function in this paper

In a general X-ray image, the blood vessel has a dark tubular structure with respect to the background, and the Hessian matrix of points in the blood vessel has an eigenvalue  $\lambda_1$  of a small absolute value and a large positive eigenvalue  $\lambda_2$ .  $\lambda_1$  is corresponding to the eigenvector along the axial direction of the blood vessel, while  $\lambda_2$  is corresponding to the eigenvector of the vertical vessel axis. These eigenvalues satisfies  $|\lambda_2| \gg |\lambda_1|$ . This paper compares some of the current vascular functions [10] - [13] and proposes a new vascular function:

$$f(p, \sigma) = \begin{cases} \arctan |\lambda_2| - 1 & \lambda_2 > c \\ 0 & \text{else} \end{cases}. \quad (4)$$

Where  $c$  is the empirical threshold based on a specific contrast environment, this paper takes  $c = 2$ . The final image output based on multi-scale enhancement is

$$f(p) = \max_{\sigma_{min} \leq \sigma \leq \sigma_{max}} (f(p, \sigma)). \quad (5)$$

Where  $\sigma_{min}$  and  $\sigma_{max}$  correspond to the minimum and maximum dimensions of the Gaussian function respectively. Since 95% of the weight of the Gaussian function is between  $[-2\sigma, 2\sigma]$ , thus we could take  $[\sigma_{min}, \sigma_{max}] = [d_{min}/4, d_{max}/4]$  [13], where  $d_{min}$  and  $d_{max}$  are respectively the minimum and maximum values of the vessel diameter in the contrast image. For the convenience of description, the enhanced graph of the output of equation (5) is referred to as vascular feature map.

Fig. 1 shows the multi-scale enhancement effect diagrams under the new vascular function and the traditional Frangi vascular function respectively. It is obvious that the new vascular function of this paper has a better enhancement effect, and the enhanced image clearly shows the contour of the blood vessel in different sizes. The vascular region is brighter, and there are fewer peripheral interference elements.

2) *Dual-stage Region Growing*: Based on the obtained vascular feature map, this paper adopts a fully automated dual-stage region growing method to extract the blood vessel contour. It is mainly divided into three processes: the automatic selection of initial seed points, the first stage of region

growing to extract the branches of the main blood vessels, and the second stage to enhance the small blood vessels. Firstly, in the automatic selection of the initial seed point, the literature [10] selects the maximum intensity point as the initial point by the corner mask processing, but does not exclude the large noise interference point in the middle of the image, which causes the initial point selection error. In this paper, the disk with the diameter  $d_{max}$  is matched to the whole image. When the sum of the intensities of all the points in the disk is the largest, the center of the disk at this time is used as the initial point of the region growing, which can effectively avoid the interference of noise points.

The contour of the main branch of the blood vessel in the contrast image is generally obvious, while the contour of the small blood vessel is blurred, and the difference from the surrounding background is small. In the process of traditional region growing segmentation, blood vessel has only a single threshold. The selection of threshold value has a great influence on the accuracy of vessel segmentation [14]. If the threshold value is small, the tiny blood vessels cannot be extracted. If the threshold value is large, the main branch of the blood vessel may be added to the interference point of the peripheral point which is bigger than the actual one. Therefore, this paper uses region growing of phased thresholds. In the first stage, a smaller threshold is selected, and the surrounding pixel points are searched from the selected initial seed point. When the surrounding pixel points satisfy the inequality  $f(p) - f_{average} < k_1$ , the points are added to the blood vessel area, where  $f_{average}$  is the average intensity of segmented blood vessel in this region. The first stage mainly divides the main branches of the blood vessels.

The second stage selects a slightly larger threshold  $k_2$ , when the surrounding pixel points satisfy the inequality  $f(p) - f_{average} < k_2$ . And the number of points around that have belonged to the blood vessel pixel point in the circular area of radius  $r$ , is at most 30% of the total number of points in the circular area. if satisfying two conditions, this point will be added to the blood vessel area. Otherwise the point is discarded. Finally, the morphological closing operation of the image can fill the small holes left in the blood vessel to smooth the contour. As can be seen from Fig. 2 (a)(b), the second-stage region growing extends the length of small blood vessels (the red circled area in the figure) without adversely affecting the main branch of the blood vessel.

### B. Skeleton Extraction and Stenosis Recognition

Common methods for skeleton extraction of images include the largest disks method [15], the fire propagation method, and the peeling method [16]. In this paper, the vascular skeleton is extracted by the Zhang-Suen algorithm based on deletion in the thinning algorithm. The algorithm defines four conditions for the pixel to be deleted, and deletes the points satisfying the condition, and finally obtains

the skeleton of the binary image. The algorithm performs efficiently and the skeleton which is obtained has no extra branches, as shown in Fig. 2(c).

To detect the location of a vascular stenosis, it is necessary to search for all points on the skeleton and calculate the diameter of the blood vessel at each point. The skeleton points extracted by the Zhang-Suen algorithm can be divided into four categories by the number  $n$  of direct connected points in eight fields. (1) When  $n = 1$ , the point is the end point of blood vessels. (2) When  $n = 2$ , the point is the intra-segment point of blood vessels. (3) When  $n = 3$ , the point is the branch point of blood vessels. (4) When  $n = 4$ , the point is intersection point of blood vessels. An example of various skeleton points is shown in Fig. 3. A direct connection point of a skeleton point and eight fields is obtained by the following conditions:

(1) The point where the four fields of the point are 1 is the direct connection point;

(2) The diagonal point of the point is 1 and the four field points of the diagonal point have no direct connection point, and the diagonal point is a direct connection point.

The vascular end points, vascular branch points, and vascular intersections on the skeleton divide the entire vascular network into different blood vessel segments. The whole search process of skeleton points is performed in a recursive manner. First, a vascular end point is randomly selected as the starting search point, and the point is used as the current search point of this blood vessel segment. Then the subsequent direct connection points of current one are sequentially calculated. If the number of direct connection points is 1, the point is added to this segment. Also the

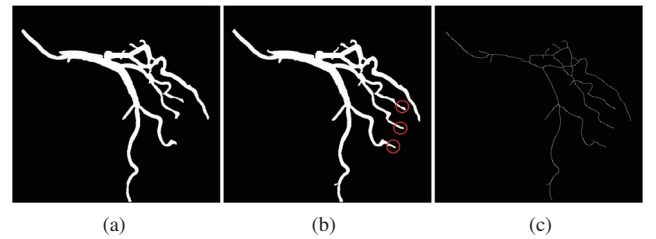


Fig. 2. Dual-stage region growing and skeleton extraction. (a) The first-stage region growing. (b) The second-stage region growing. (c) Skeleton extraction of blood vessels

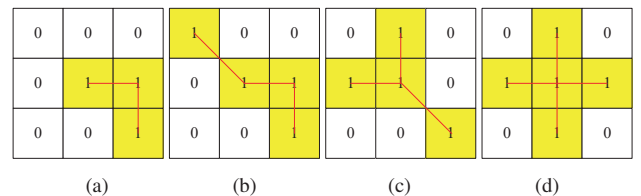


Fig. 3. Examples of various skeleton points. (a) $n=1$ , the end point. (b) $n=2$ , the intra-segment point. (c) $n=3$ , the branch point. (d) $n=4$ , the intersection.

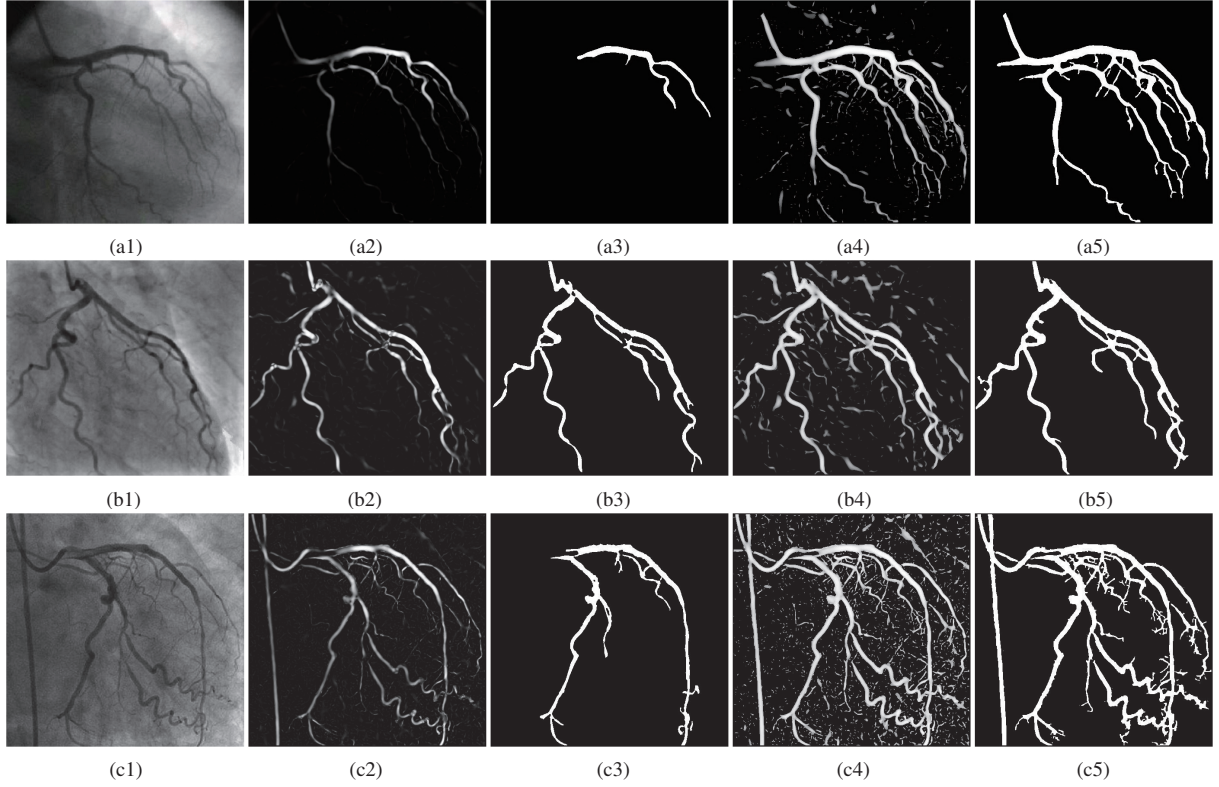


Fig. 4. Comparison of vascular enhancement and segmentation effects. (a1), (b1) and (c1) are three original angiographic images. (a2), (b2) and (c2) are the enhancement effects of Frangi vascular function. (a3), (b3) and (c3) are respectively the result of the growing of single threshold region of (a2), (b2) and (c2). (a4), (b4) and (c4) are the enhancement effects of vascular function in this paper. (a5), (b5) and (c5) are respectively the results that (a4), (b4) and (c4) are handled by phased regional growth in this paper.

subsequent direct connection point is used as the current point to continue searching. Second, if the number of subsequent direct connection points is greater than or equal to 2, a new search is performed for each subsequent direct connection point until all points on the skeleton have been searched. Third, for each skeleton point, calculate the maximum disk diameter at which the point is centered and all points in the circle are within the vessel. And the calculated result is taken as the diameter of the vessel at this point.

Through the above process, the different vessel segment numbers corresponding to each skeleton point and the blood vessel diameter there are obtained. In the angiographic image, Blood vessels have many interlaced branches, forming a complex network, and it is difficult to identify the obstruction position of the diseased blood vessel integrally. Since vascular obstruction occurs mostly in the main branch, and the judgment of vascular stenosis is compared with the diameter of the anterior and posterior vessels, this paper uses the method of phased judgment to automatically diagnose. For the obtained No.  $i$  vascular segment, the average diameter  $D_{min}^i$  and the minimum diameter  $D_{min}^i$  of this segment are calculated separately. According to the criterion of literature

[17], whether the vascular is obstructed in this segment could basically satisfy the following formula which has been adjusted:

$$\begin{cases} 0.45 < D_{min}^i / D_{avg}^i < 0.75 & \text{General obstruction} \\ D_{min}^i / D_{avg}^i \leq 0.45 & \text{Severe obstruction} \end{cases} \quad (6)$$

If the blood vessel segment  $i$  is a obstruction blood vessel, the position of minimum diameter  $D_{min}^i$  on the blood vessel is the obstruction point. The obstruction is generally divided into two levels, general obstruction and severe obstruction, and different levels of stenosis are circled with different colors in the experimental images.

### III. EXPERIMENT

The experiment is divided into two parts, one is angiographic image enhancement and vessel segmentation, and the other is automatic extraction of skeleton extraction and vascular stenosis. The angiographic images in the experiment were from a medical website (<http://www.cmt.com.cn/>), and the experiment was programmed with Matlab R2018a.



### A. Vessel Segmentation Experiment

Vessel segmentation experiment was compared with the vascular contour map obtained by the single threshold region growing on the vascular feature map using the Frangi algorithm to verify the effectiveness of the vessel segmentation method in this paper. Fig. 4 shows the comparison of the experimental results of the three contrast images. It can be clearly seen that the vascular feature map obtained by Frangi vascular function has a higher response in the large vessel region and a weaker response at the small vessel and the vessel edge. So that only the outline of the large blood vessels can be obtained on this basis. The vascular feature map obtained by the new vascular function of this paper has obvious vascular contours, and the large and small blood vessels are well enhanced. The vascular region has high brightness and few interference elements around it. On the basis of this, the dual-stage region growing adopted in this paper obtains a good blood vessel contour. The accurate contours of the relatively clear large blood vessels in the contrast image are extracted accurate contours, and the fuzzy small blood vessels performs well in the second region growing. The experimental results show that the vessel segmentation method in this paper is much better than the method using Frangi algorithm and single threshold region growing.

### B. Automatic Diagnosis of Vascular Stenosis

Several angiographic images of lesions and stenosis which are diagnosed by doctors are applied in the experiment. The positions of vascular stenosis in these images are circled by the automatic diagnosis method of this paper, comparing with the positions of vascular stenosis marked by the doctor. Three representative images with vascular stenosis are shown in Fig. 5. It can be seen that Fig. 5(a3) in which there are clear blood vessels and few small branches, can be accurately identified, and there is no redundant misdiagnosis point. In many complex angiographic images with many small vessel branches, the location of the obstruction marked by the doctor is detected. Moreover, other suspected vascular stenosis positions were circled.

Here two evaluation indicators for vascular stenosis detection are used: recognition rate and accuracy rate. The recognition rate refers to the ratio that the number of stenosis points automatically diagnosed which is positive account for the total number of points circled by the doctor. While the accuracy rate refers to the ratio that the number of stenosis points automatically diagnosed which is positive account for the total number of lesion points circled by the automatic diagnosis. In this paper, 10 angiographic images with obvious obstruction were tested. The results showed that the total lesion recognition rate was 80% and the effective rate was about 50%. The efficiency of automatic diagnosis is low, and misidentification occurs mostly at the end, corner

and branch of the vessel segment. The reason is that there are more interfering elements in these positions, and the contour of the blood vessel deviates from the tubular shape, and the effect of enhancement based on Hessian matrix is unsatisfaction and the measured diameter of blood vessel is too small. Although the accuracy of automatic diagnosis needs to be improved in some aspect, but the recognition rate of positive lesions is high. The automatic diagnosis of this paper may be used as a pre-diagnosis before the final judgment of the doctor, and most suspected vascular stenosis can be found through pre-diagnosis. Then, based on the pre-diagnosis results, doctors can eliminate some interference points, and the position of positive vascular stenosis can be found quickly and accurately, which greatly reduces the workload of doctors. Furthermore, pre-diagnosis can quantify the diameter of the blood vessel, and doctors can get a curve of the diameter of blood vessels on the segments they are interested in, so as to facilitate further analysis and diagnosis of the vascular lesion.

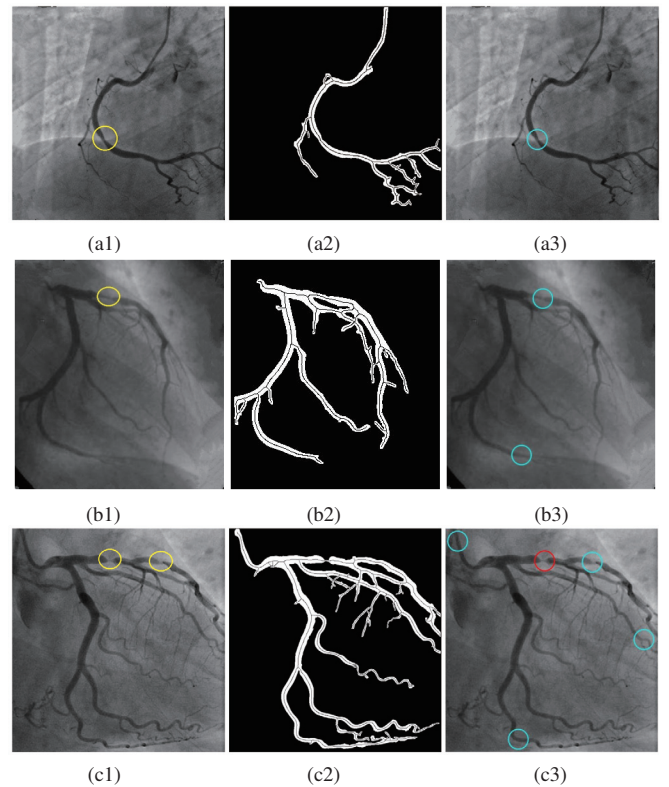


Fig. 5. Results of automatic diagnosis of vascular stenosis. (a1), (b1) and (c1) are three original angiographic images, and the yellow circle is the narrow position of the blood vessel circled by the doctor. (a2), (b2) and (c2) are the contour and skeleton of blood vessels extracted by this method. (a3), (b3) and (c3) are the narrowness of blood vessels circled automatically in this paper. Blue one indicates general obstruction and red one indicates severe obstruction.

#### IV. CONCLUSION

In this paper, a new vascular function based on multi-scale enhancement of Hessian matrix is adopted, and the contour of blood vessels is extracted by a dual-stage region growing segmentation method on the enhanced vascular feature map. On this basis, vascular skeleton extraction and diameter measurement are performed to achieve a fully automated pre-diagnosis of vascular stenosis. The experimental results show that in the multi-scale image enhancement stage, the new blood vessel function employed in this paper can make the blood vessel contour more obvious and with less interference. Using the automatic detection of seed points and the dual-stage region growing method, the contours of the main branches of the extracted vessels are accurate, and the small blood vessels are also well enhanced and segmented. A fast and fully automatic pre-diagnosis of the extracted blood vessel contour is achieved, and the diagnosis may provide auxiliary reference and quantitative basis for the doctor's final judgment. However, there are still some limitations. Due to the interference factors of the end, corner and branch of the vessel segment, the efficiency of automatic diagnosis needs to be further improved. In future research, the vessel segmentation algorithm will be optimized. Furthermore, angiographic image sequence will be taken into consideration to improve the segmentation effect of tiny blood vessels and better automatic diagnosis effect.

#### ACKNOWLEDGMENT

This work was greatly supported by the National Natural Science Foundation of China (Grant No. 61973210), Shanghai Science and Technology Commission (Grant No. 17441901000), the Medical-engineering Cross Projects of SJTU (Grant Nos. YG2019ZDA17, ZH2018QNB23), and the Scientific Research Project of Huangpu District of Shanghai (Grant No. HKQ201810).

#### REFERENCES

- [1] S. Hu, R. Gao, L. Liu et al., "Summary of the 2018 report on cardiovascular diseases in China," *Chinese Circulation Journal*, vol. 34 No.3, pp. 209-220, March, 2019.
- [2] A. Lasso and E. Trucco, "Vessel enhancement in digital X-ray angiographic sequences by temporal statistical learning," *Computerized Medical Imaging and Graphics*, vol. 29, no. 5, pp. 343-355, August 2005.
- [3] C. Kirbas and F. Quek, "A review of vessel extraction techniques and algorithms," *ACM Computing Surveys*, vol. 36, no. 2, pp. 81-121, December 2004.
- [4] Y. Li, X. Li, Z. Lu and W. Huang, "Vessel segmentation of fundus image based on Markov random field," *Computer Applications and Software*, vol. 36, no.7, pp. 254-258+306, July 2019.
- [5] T. Lv, G. Yang et al., "Vessel segmentation using centerline constrained level set method," *Multimedia Tools and Applications*, vol. 78, no. 2, pp 17051-17075, January 2019.
- [6] S. Roy, A. Mitra, S. Roy and S. K. Setua, "Blood vessel segmentation of retinal image using Clifford matched filter and Clifford convolution," *Multimedia Tools and Applications*, August 2019, DOI: 10.1007/s11042-019-08111-0, [Online].
- [7] Q. Li, B. Feng et al., "A Cross-Modality Learning Approach for Vessel Segmentation in Retinal Images," *IEEE Transactions on Medical Imaging*, vol. 35, no. 1, pp. 109-118, January 2016.
- [8] H. Fu, Y. Xu et al., "Retinal vessel segmentation via deep learning network and fully-connected conditional random fields," *2016 IEEE 13th International Symposium on Biomedical Imaging (ISBI)*, pp. 698-701, 2016.
- [9] J. Chen, L. Zhao, D. Li and T. Wan, "Automated detection and quantification of coronary artery stenoses based on vessel tree segmentation in X-Ray angiography," *Chinese Journal of Biomedical Engineering*, vol. 38, no.3, pp. 266-272, June 2019.
- [10] T. Y. Zhang and C. Y. Suen, "A fast parallel algorithm for thinning digital patterns," *Communications of the ACM*, vol. 27, no. 3, pp. 236-239, March 1984.
- [11] T. Wan, X. Shang et al. "Automated coronary artery tree segmentation in X-ray angiography using improved Hessian based enhancement and statistical region merging," *Computer Methods and Programs in Biomedicine*, vol. 157, pp. 179-190, April 2018.
- [12] C. Mei, L. Wu, Y. Yang et al., "An approach for segmentation of X-ray angiographic image based on region growing and structure inferring," *Journal of Biomedical Engineering*, vol. 31, no. 2, pp. 413-420, April 2014.
- [13] L. Chen, "Researches on vessel image enhancement based on Hessian matrix and level-set segmentation algorithm," M.S. thesis, Hunan Univ., Changsha, China, April 2012.
- [14] I. A. Tache, "Vessel segmentation of coronary X-ray angiograms," *2016 20th International Conference on System Theory, Control and Computing (ICSTCC)*, Sinaia, pp. 727-731, 2016.
- [15] D. Nain, "An interactive virtual endoscopy tool with automatic path generation," M.S. thesis, Massachusetts Institute of Technology, Cambridge, MA, USA, May, 2002.
- [16] X. Wang, Y. Wu, H. Mao and B. Tian, "Analysis and application of iteration skeletonization algorithm in recognizing Chinese characters image," *Journal of Liaoning University*, vol.40, no. 3, pp. 227-232, August 2013.
- [17] H.A. Kirişli, M. Schaap, "Standardized evaluation framework for evaluating coronary artery stenosis detection, stenosis quantification and lumen segmentation algorithms in computed tomography angiography," *Medical Image Analysis*, vol.17, pp. 859-876, 2013.